A Survey of Free Space Optical Communications in Satellites

AE 8900 MS Special Problems Report
Space Systems Design Lab (SSDL)
Guggenheim School of Aerospace Engineering
Georgia Institute of Technology
Atlanta, GA

Author:
Stephen Hall

Advisor:
Prof. Brian C. Gunter

May 3, 2020

A Survey of Free Space Optical Communications in Satellites

Stephen Hall
School of Aerospace Engineering
Georgia Institute of Technology
Email: shall68@gatech.edu

***Abstract*—Free space optical (FSO) communications is an up and coming set of technologies that promises significantly higher data rates at lower size, weight, and power than currently achievable by RF communications. FSO communications in satellites has been a subject of research for decades. It is strongly believed that FSO communications will be incorporated in next generation communications relay satellites and that FSO communications will enable new types of interplanetary missions previously infeasible due to bandwidth or power restrictions. FSO technologies are becoming mature enough to be fielded for use and represent a complex trade space of new components and technologies. This paper presents an overview of concepts in satellite FSO communications including deep space communications, pointing, cloud coverage, modulation, and detection, and discusses the current devices and technologies that enable FSO communications.**

I. Introduction

FREE space optical (FSO) communications is a class of line-of-sight communications technology that wirelessly transmits information by means of modulated light [1]. NASA mission modeling indicates a desire for a ten times improvement in data rate for each decade through 2040 [2]. Currently, an image from the Mars Reconnaissance Orbiter (MRO) takes around 1.5 hours to transmit back to Earth with its maximum data rate of 6 Mbps [3], which is clearly not suitable for future (especially crewed) missions to Mars. As the demand for faster satellite communication rates increases and the RF spectrum becomes more congested [4], new and improved methods of satellite communications become more and more necessary. Future FSO communication technologies promise this. Compared to their RF counterparts, FSO communication systems have much higher bandwidth available allowing for faster data rates on the order of many Gbps [5]. RF communications operate at wavelengths of around 1 cm and above, and optical communications use electromagnetic beams with wavelengths orders of magnitude smaller: around 1550 nanometers and below. Electromagnetic beam divergence is proportional to λ/D, where λ is a wavelength and D is an aperture diameter [6]. A smaller wavelength therefore implies a more directional beam and a smaller required aperture. As a result, FSO systems require smaller antennas, can be lighter in weight, and require less power when compared to traditional RF communication systems, making FSO technology beneficial in terms of size, weight, and power (SWaP) for satellite missions. The high directionality of FSO communications provides immunity from electromagnetic interference. Narrow, directional beams also imply increased security as they are resilient to jamming or interception. Intercepting an FSO communication requires being in the line-of-sight, whereas RF communications are easily intercepted and rely heavily on encryption methods for information security. Furthermore, in contrast to RF communications where band congestion and frequency coordination present significant problems, the narrow and directional nature of FSO communications provides a license-free band that may never need to be regulated [1].

Satellite FSO communication occurs by using lasers to carry information. The laser beam travels some distance and is collected by a receiving telescope which focuses the laser beam onto a detector. The detector converts the inbound light into electrical signals that are further processed to recover the information embedded on the laser beam. There are several challenging aspects of implementing this type of system. Though not comprehensive, this paper aims to provide a broad overview of these concepts and challenges. Section II discusses the concept of operations of an FSO communications system and identifies special considerations for space-to-ground and deep space FSO communications. Then, several existing satellite FSO demonstrations are surveyed in section III. The loss associated with mis-pointing a laser beam and mechanisms utilized for maintaining pointing quality from FSO communication satellites are discussed in section IV. FSO communication receivers and modulations are discussed in section V, including photodiodes, photon counting, adaptive optics, and optical detection techniques.

II. Concept of Operations

The basic concept of operations for optical communications, as in traditional RF communications, is to transfer some amount of data at the source to the destination with as little corruption as possible. In satellite communications, the communication process is scheduled to start at a specific time slot that is governed by orbital geometry. At the beginning of the slot, some link acquisition process occurs. Data is then transferred until no more data remains or the end of the time slot is reached [3]. The narrow beam divergence inherent in optical communications drives the need for significantly better pointing precision when compared to the pointing required for traditional RF communications. Typical requirements may be on the order of a few hundred μrad [7]. This level of pointing accuracy will typically go beyond what the host spacecraft

body pointing is capable of and special operations or extra gimbal/steering mechanisms will need to be utilized to achieve the necessary pointing. Further, a narrow beam implies an unregulated band. Spacecraft utilizing optical communications will not need to worry significantly about interfering with each other's transmissions as a very fine pointing lock is needed. As a result, each spacecraft can utilize as much bandwidth as they could reasonably need. In RF communications, modulation schemes represent a trade off between bandwidth and power efficiency. Being more bandwidth efficient generally means a higher power requirement for reliable communication [8]. Depending on the situation, either bandwidth or power efficiency might be more important. With a wide bandwidth available for use in optical communications, the primary concern need never be efficient bandwidth use. Modulation schemes can be chosen to reduce the power requirement without concern for the bandwidth qualities of the modulation.

As previously mentioned, FSO communications are realized by using a light source to transmit information. In satellite FSO communications, the light source will typically be a laser that is fed through some transmit optics, travels through free space and/or the atmosphere, is collected by a receiving telescope, and is converted into an electrical signal and decoded. A link budget can utilized to characterize the link and inform design decisions. The link budget contains information on power gain and loss factors that the laser will encounter before reaching the receiver. That is,

$$P_r = GP_t \tag{1}$$

where P_r is the power received, P_t is the power transmitted, and G is a total gain/loss factor that accounts for all gains and losses in the laser's path. G can be split up into many different components of the system depending on how detailed of an analysis is needed. An example is [9]:

$$G = G_t\eta_t L_s L_p G_r \eta_r \eta_D \tag{2}$$

where G_t and η_t represent the gain and efficiencies of the transmitter optics, L_s represents free space path loss, L_p represents pointing loss, G_r and η_r represent the gain and efficiency of the receiving optics, and η_D represents a truncation error that captures the effect of the receiver only capturing a portion of the transmitted light that, at orbital distances, will have a much wider footprint than the receiving telescope's aperture. Numbers associated with transmitter and receiver efficiencies or gains will clearly be implementation dependent, and could include effects such as gain associated with lowering the divergence of the beam, or flaws such as loss in relay optics. L_s can be approximated by the inverse square law associated with the geometric spread of light [9]:

$$L_s = (\frac{\lambda}{4\pi R})^2 \tag{3}$$

with λ being the wavelength and R being the distanced traveled. Several ways to approximate L_p, and a method for approximating L_p, L_s, and η_D together are discussed in depth in section IV-A. This not the only way to form a link budget, of course. Many different parameters could be taken into account, or some can be ignored or loosely approximated. Tabulating systematic gains and losses will help provide insight into the system and can be used as a design tool.

The realization of the operations involved in FSO communications will depend on several factors, some of which will certainly be mission specific. In the subsequent sections, space-to-ground and deep space FSO communications are discussed. In each scenario, different considerations need to be made based on the atmosphere, cloud cover, pointing requirements, orbital geometries, choice of modulation, and more.

A. Space-to-Ground

Associated with a space-to-ground link is optical transmittance through the atmosphere. Importantly, atmospheric effects serve only to hinder the transfer of data from space-to-ground or vice versa. Overcoming these hinderances requires some addition of complexity in the transmitter, receiver, or both. The complexity of the instruments on the spacecraft are of concern, as a more complex optical transmitter represents a greater cost to build and launch the spacecraft and also a greater risk that the system won't work as planned. Conversely, the complexity of an optical ground station is less of a concern because we are not limited by the complexity of the systems and structures we can build on the ground. This is not a new concept, and it is also seen in RF communications. The existing ground architecture for the Deep Space Network (DSN) consists of colossal 34m and 70m antennas that have been operational for over 40 years [10]. Constructing, maintaining, and upgrading this scale of construction is reasonably possible on the ground and impractical in space. Just as in radio communications, the antennas (telescopes) used in FSO communications will be limited on the spacecraft. Because complexity of a ground system can be virtually infinite, the scale of the optical ground stations will be adjusted to compensate.

Like the DSN, multiple optical ground station sites will need to be available in order to ensure good coverage. The DSN currently consists of three sites: Goldstone, California; Madrid, Spain; and Canberra, Australia. With these three sites, the DSN achieves greater than 99% coverage for deep space satellites [11]. Radio communications can very easily propagate through cloud coverage. With three stations, the DSN can achieve this coverage 24/7. Unlike radio communications, it is impossible for most types of cloud coverage, with the exception of high semitransparent (cirrus) clouds [12], for optical communications to pass through clouds. The placement of optical ground stations therefore has another factor to consider to successfully achieve geographic diversity: the cloud free line of sight (CFLOS) probability of the ground station. CFLOS probability estimation for a single optical ground station or a network of optical ground stations has been an area of study in [12]–[19].

A common way to analyze an optical space-to-ground link is to consider the channel availability as a Bernoulli random variable. That is, the channel is "on" with some probability p, and "off" with probability $1-p$. This adequately captures cloud coverage and other atmospheric effects can be taken into account after the fact. The probability that the channel is available when the satellite of interest is in view is the

CFLOS probability, and determining it is a challenge. The probability that a ground station is available depends both on the location of the ground station and the location of the satellite in question. [16] and [15] present methods for estimating the availability of an optical ground station or, since cloud coverage between sites cannot necessarily be considered independent, a network of spatially correlated optical ground stations. Satellite slant angle is taken into account in [16] by including cloud data for the highest possible cloud at the lowest possible telescope elevation in the estimation for p. [12]–[16] utilize cloud coverage data products from a variety of existing satellites including the GOES and Meteosat series of satellites, CALIPSO, and others in order to determine the CFLOS probability. In particular, the cloud fraction data product from NASA's Terra and Aqua satellites [20] is utilized by [16]. [12] finds that if the link budget that is used to determine optical ground station (OGS) availability includes attenuation for high altitude semi-transparent clouds, the optimum number of OGSs is not reduced but the number of handovers needed is reduced by 20%. Other costs associated with setting up ground infrastructure may be influential, and [14] attempts to optimize OGS location while considering the cost to stand up the backbone network between them. For deep space missions, [13] shows that a six station OGS network (OGSN) can achieve 90% availability using monthly and yearly meteorological variations. [12], [14], [15], [17], [19] all consider yearly averages to determining OGS selection. [13] includes monthly availability in OGS selection and [14] and [12] show average monthly availability of ground stations. Monthly average cloud coverage can change drastically, and there are also great variations in monthly cloud coverages in the two hemispheres [18]. For adequate temporal resolution in the selection of OGS placement, monthly cloud coverage statistics should be considered during optimization.

More recently, stochastic dynamic models for generating integrated liquid water content (ILWC) fields have been developed and used to determined CFLOS probability [17]–[19]. A set of multidimensional stochastic differential equations (SDEs) is used to synthesize an ILWC time series, which is correlated both spatially and temporally. The resulting model along with microphysical properties of clouds can be used to synthesize a space-time model of cloud attenuation, resulting in the synthesis of a 3D cloud field [17]. [19] employs cloud field synthesis with ILWC statistics to generate a CFLOS probability time series for satellites, taking into account both the changing elevation angle of a non-GEO satellite and the elevation of the optical ground station. Yearly and monthly ILWC statistics can be approximated as log-normal distributions [18] and data for modeling them is readily available.

B. Deep Space

The farthest FSO demonstration to date has been the Lunar Laser Communications Demonstration (see III-E). For communications purposes, this is still considered near Earth. Deep space communications in this context will refer to anything beyond lunar distances, although different organizations have defined deep space to start at varying distances from Earth. Achieving optical communications in deep space requires some extra considerations. Complications arise from planetary distances in the form of varying and long light times, low Sun angles, large path loss, and strict pointing requirements. The Mars Laser Communication Demonstration (MLCD) was planned to be the first deep space optical communications relay to be flown on the Mars Telecom Orbiter (MTO) in 2009 [21]. Although program changes resulted in the cancellation of the MTO and thus the MLCD, the project completed preliminary design reviews for both flight and ground systems [22]. Having achieved significant conceptual development, the MLCD can be used to study the unique requirements of deep space optical communications. The MLCD was designed to demonstrate 10-30 Mbps downlink in favorable conditions, and at least 1 Mbps in the worst conditions. To achieve this, 64-ary pulse position modulation (64-PPM) was to be used. A Mach-Zehnder modulator, a component similar to those that are pervasive in the fiber optic telecom industry, would accomplish this [21]. The design of the MLCD to achieve these communications goals includes consideration for many of the things that make deep space optical communications challenging: path loss, doppler shift, light time, pointing loss, and Sun angle. Subsequent discussion of these concepts will relate back to the MLCD design where possible.

Of prime concern in deep space optical communications are the shear distances involved that result in large free space path losses. As is familiar in RF communications, FSO communications also experience a $1/R^2$ power penalty due to beam propagation geometry. As an example, figure 2 shows that the distance between Earth and Mars varies between approximately 0.5 and 2.5 AU over time due to orbital geometries. Relative to a geosynchronous orbit (≈ 0.00023 AU), a Mars probe would experience a 65-80 dB path loss penalty depending on distance between the two planets. The link budget for optical terminals will need to incorporate the worst case scenario distance. This could be accomplished, for example, by utilizing larger antenna apertures in the the optical terminal design or by utilizing variable coding/modulation rates. The MLCD was designed to utilize variable data rates and planned to operate at the minimum rate of 1 Mbps at this distance as a compensatory measure for increased path loss.

Deep space optical communications must also consider long light times and doppler shift due to planetary distances and large relative velocities. Long light times limit the types of interactions that can be had between a ground station and a spacecraft. The light time between Earth and Mars varies between approximately 4 and 20 minutes. With the round trip signal being greater than 10 minutes most of the time, FSO acquisition strategies that work near Earth will not be suitable for deep space missions. Beacon aided pointing has been employed by many FSO missions (see III). This concept involves a ground station emitting a reference beam that the spacecraft finds and then tracks. The simplest manifestations of this, such as the spacecraft scanning in some pattern to acquire the beacon, rely on near zero light time between the ground and the spacecraft. This and other interactive acquisition strategies that work near Earth will not work near Mars when the time to communicate with the spacecraft is on the order of

minutes. The acquisition process for the MLCD was planned to work around these issues by using a combination of Earth image tracking and a modulated uplink beacon [21].

Long light time necessitates the use of a lookahead angle for optical transmissions. An optical terminal at Mars needs to point at where the Earth will be when the signal arrives, not where it is currently. This effect is captured with a lookahead angle. The lookahead angle is an angular offset by which the optical beam must be steered when the optical head is pointed at where Earth currently is. At planetary distances, the lookahead angle will be larger than the optical beam's divergence. The point ahead angle can be expressed as $2v_{transverse}/c$, where $v_{transverse}$ is the transverse velocity of the probe relative an Earth observer, and c is the speed of light. In the example of a Mars probe, the maximum lookahead angle occurs at planetary opposition and is approximately 347 μrad [23]. The lookahead angle varies as the distance and, therefore, the relative velocities between the two planets vary. The minimum lookahead angle for Mars occurs at planetary conjunction and is around 20 μrad. The maximum lookahead angle would be, for the MLCD, well over 100 times the beam width of the optical terminal, and an accuracy of a fraction of a beam width would be needed for sufficient pointing [24]. The MLCD design uses a separate precision steering mirror within the optical head to achieve the desired lookahead angle. A fraction of the light from the transmit beam is redirected to a focal plane array (FPA) which also tracks light reflected by Earth for coarse steering. The lookahead mirror then steers the centroid of the transmit beam to be the correct distance from the Earth centroid on the FPA corresponding to a pre-calculated lookahead angle [22].

Another property resulting from the large relative velocities inherent with planetary distances is doppler shift. Generally, a bandpass filter is required at the receiver of an optical link to receive as much of the desired wavelength as possible while rejecting other incident light. This is especially important for Earth based receivers where atmospheric scatter of sunlight and other light sources can significantly raise noise levels. As a result, a filter with a very narrow bandwidth, on the order of 0.05 nm, is desirable to limit this noise. [6]. At planetary distances and speeds, doppler shift of the received light can shift the received frequency beyond these filter limits. Doppler shift can be expressed as v_{range}/c, where v_{range} is the range rate of the optical transmitter relative to the observer. At Mars, the observed wavelength will be shifted by 0.07-0.1 nm, which must be accounted for when designing the receivers filter [23].

When discussing background noise due to the Sun, a primary factor to consider is how close to the Sun the optical transceiver is pointing. In deep space, this is an important factor to consider, as geometry may dictate total link outages lasting weeks to months due to the Sun being too close to the direction the receiver needs to point. Two angles are defined to describe the location of the Sun relative to the link direction: The Sun-Earth-Probe (SEP) and the Sun-Probe-Earth angle. The SEP and SPE angles define how far the Sun is relative to the optical line of sight that defines the link between a space based probe (e.g, an optical communications terminal) and an Earth observer. In this discussion, an Earth observer includes any Earth based receiver including both ground stations and Earth orbiting satellites. Figure 1 shows the definition of the SPE and SEP angles using a Mars based probe as an example. The lower the SEP and SPE angles are, the more closely the optical transceiver is pointing toward the Sun: 0° being directly at the Sun and 180° being directly away from the Sun. An SEP or SPE angle greater than 90° indicates that the optical terminal points into the night sky to maintain line of sight, and an angle of less than 90° would point into the daytime sky. The lower the SEP or SPE angle, the more background noise an optical receiver will get from the Sun. For most outer planets, an Earth observer will spend approximately 10% of the time at a Sun angle below 10° and 1-5% of the time at a Sun angle below 3°. Conversely, a probe at an outer planet will spend less than 10% of the time with an SPE angle less than 10° with this percentage increasing up to 100% the further out the planet is. For example, the SPE angle for a probe at Pluto will be less than 2° 100% of the time. Further characterization for the amount of time spent at varying low Sun angles for several planets and Lagrange points can be found in [25].

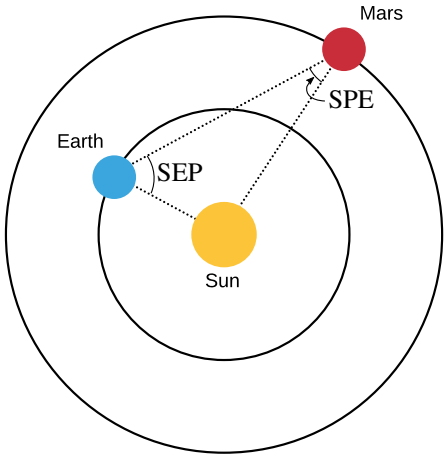

Fig. 1. Sun-Earth-Probe (SEP) and Sun-Probe-Earth (SPE) angle illustration for a Mars based probe. Also see [21], [23]

Figure 2 shows an example of the variation SEP and SPE angles over time due to orbital geometries. At opposition, Earth and Mars are at their farthest distance from one another and on opposite sides of the Sun. In order for a ground terminal to point at a Mars based terminal at this time, it will have to point near the Sun as well. At opposition, the Mars probe will also have to point near the Sun to look at the Earth based terminal . At conjunction, Earth and Mars are closest to one another and both planets are on the same side of the Sun. Because Mars is an outer planet, an Earth based terminal looks away from the Sun into the night sky to point at a Mars based probe, corresponding to a SEP angle approaching 180°. The Mars based probe will point into the Sun to look at an Earth based terminal. The trend between SEP and SPE at planetary opposition/conjunction is reversed when considering an inner planet instead. Thus for outer planets, an Earth based terminal takes a large receive penalty due to increased background noise from the Sun at planetary opposition, and the outer

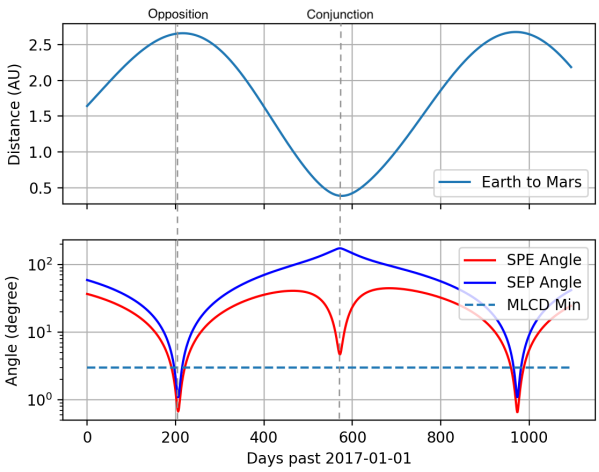

Fig. 2. Mars to Earth distance and corresponding SEP/SPE angles. Generated using Earth and Mars ephemerides from JPL's HORIZONS system [26]

planet probe takes a similar penalty at both opposition and conjunction. Considering the Mars scenario, it's seen in Figure 2 that the SEP angle is below 90° most of the time. Mars is primarily observable from the daytime sky, and the ground infrastructure must accommodate the background noise from the Sun. The MLCD was planned to demonstrate the worst case scenario by working with SEP angles down to 3° at a reduced datarate of 1 Mbps [22]. Figure 2 shows this limit, indicating that there would still be fair lengths of consecutive time (25 days [21]) where the MCLD would experience total link outage.

III. Satellite FSO Missions

This section presents existing satellite missions that implement an FSO communications link. Table I contains a list of these missions and associated references. There have been a fair amount of experimental FSO missions that have flown to date and Table I is not comprehensive. Several of the included satellites are, however, iconic. GOLD, was the first satellite based FSO communications experiment and was operated in partnership between JAXA and NASA/JPL. The fastest satellite based FSO communications experiment to date achieved 5.6 Gbps in bidirectional communication between two TESAT laser communication terminals (LCTs) hosted on the NFIRE and TerraSAR-X satellites in LEO. Recently, NASA's LLCD achieved the farthest space-to-ground optical downlink at 622 Mbps from Lunar orbit, and NASA's LCRD is planned to operate as a 1.2 Gbps optical relay satellite in GEO. Table II summarizes modulation and data rate information for the surveyed missions. Based on past and presently planned missions, there is a clear interest in establishing optical communications as a viable communications method. In the remainder of this section, the experiments listed in Table I are discussed at a high level.

A. GOLD - Ground-to-Orbit Lasercom Demonstration

The Ground-to-Orbit Lasercom Demonstration (GOLD) was conducted between the ETS-VI spacecraft and JPL's optical ground station at Table Mountain [29]. ETS-VI was a NASDA (now named JAXA) owned spacecraft. From 1995-1996 ,the GOLD experiments were performed. GOLD demonstrated the first successful LEO-ground optical communications. Beacon aided pointing was used for this experiment. All of the other surveyed experiments also use this technique where an optical ground station emits a high powered beam toward the spacecraft which the spacecraft then uses as a pointing reference. GOLD used a quadrant photodetector for tracking the ground beacon and a two-axis gimbal with a fine pointing mirror for fine tracking. An 830 nm laser was used for the downlink with an output power of 13.8 mW [28]. Of this transmitted power, only approximately 2.5 nW was received at the ground station telescope. GOLD successfully demonstrated a downlink of 1.024 Mbps 2-PPM modulated data with additional telemetry about the system downlinked via S-band radio [27].

B. TESAT's LCT - Laser Communication Terminal

Under contract with the German DLR, the company TESAT developed a homodyne binary phase shift keying (BPSK) optical transceiver for space based FSO communications called the Laser Communications Terminal (LCT). The LCT was designed to be an off the shelf commercial optical communications solution [34]. The LCT was flown on two satellites: U.S.A owned NFIRE and Germany's TerraSAR-X. An inter-satellite link was established between the two LCT terminals for the first time on February 21st 2008, and a LEO-LEO FSO link was demonstrated at 5.6 Gbps [33]. Homodyne BPSK, further discussed in Section V is unique in that it provides total immunity from background radiation due to the Sun. The LCT weighed 35kg, consumed 120W of power, and was capable of establishing an inter-satellite link at distances of 1,000 - 5,100 km with a bit error rate of less than 10^{-9}. The LCT was also used to successfully communicate with an optical ground station in Hawaii at the same rates [33].

C. SOTA - Small Optical TrAnsponder

The SOTA instrument was developed by National Institute of Information and Communications Technology (NICT), with the main objective of establishing an optical communications link between space and ground. Being designed for 50-kg class satellites, SOTA weights $5.9\,\mathrm{kg}$ and employs four lasers. Two are used for communication and are operated at $976\,\mathrm{nm}$ and $1549\,\mathrm{nm}$. Two other lasers in the $800\,\mathrm{nm}$ band are used for polarization measurements. A $1064\,\mathrm{nm}$ laser is used for uplink. The uplink laser is also used as a beacon which SOTA tracks using a quadrant photodetector and fast pointing mirror for precise pointing. SOTA uses non-return-to-zero on-off-keying (NRZ-OOK) modulation with options to toggle between various types of error correcting codes. [43]

RISESAT, a Tohuko University 50kg class satellite project is hosting a variant of SOTA, VSOTA (Very Small Optical Transponder), which was also developed by NICT. Unlike SOTA which possessed a dedicated gimbaling system,

TABLE I
SUMMARY OF SURVEYED FSO MISSIONS

Mission/Instrument	Year	Type	Agency	Remark	References
GOLD	1995	GTO-Ground	JAXA (then NASDA)	First satellite FSO demonstration	[27]–[30]
LCT	2008	LEO-LEO LEO-Ground	TESAT/DLR	Fastest FSO link to date	[31]–[34]
LLCD	2013	Lunar-Ground	NASA	Farthest FSO link to date	[35]–[39]
SOTA	2014	LEO-Ground	NICT	Built for 50kg class satellites	[40]–[45]
OPALS	2014	LEO-Ground	NASA	ISS hosted	[7], [46]–[50]
LCRD	2020 (future)	GEO-Ground LEO-GEO GEO-GEO	NASA	Demonstration for next generation relays	[3], [51]–[53]

TABLE II
MODULATION AND DATARATE OF SURVEYED MISSIONS

Mission	Forward Modulation	Forward Datarate (Mbps)	Return Modulation	Return Datarate (Mbps)
GOLD	-	-	2-PPM	1
LCT	Homodyne BPSK	5600	Homodyne BPSK	5600
LLCD	4-PPM	20	16-PPM	622
SOTA	-	-	NRZ-OOK	10
OPALS	-	-	OOK	50
LCRD	4-PPM DPSK	20 1288	16-PPM DPSK	622 1288

VSOTA's optics are fixed to the satellite structure. The VSOTA instrument also uses NRZ-OOK modulation, and utilizes both a 980 nm and 1540 nm wavelength for downlink. Because VSOTA does not have a gimbal mechanism and the beams are very narrow, RISESAT must achieve pointing accuracy of 0.1 degree (3σ) to use the 980 nm channel and 0.04 degree (3σ) to use the 1540 nm channel. With limitations on pointing, output power, and ground equipment, it is expected that the downlink rate of VSOTA will be 100 kbps [41]. RISESAT launched in January, 2019. As of writing, there are no publications on the results of VSOTA.

D. OPALS - Optical Payload for Lasercomm Science

OPALS was an ISS hosted FSO experiment aimed at downlinking a video at modest rates to the Tabletop Mountain optical ground station in California. The goal of OPALS was not to improve on the state-of-the-art optical communications technology but rather to increase experience in key challenges of the field, focussing on atmospheric turbulence characterization, link availability, and pointing performance. A $1550\,\mathrm{nm}$, $1.6\,\mathrm{mrad}$ divergence beam was used for downlink and a $976\,\mathrm{nm}$ ground beacon was used for acquisition, tracking, and pointing. During optical links, the OPALS flight system downlinked a pre-coded video file using on-off-keying (OOK) modulation. The concept of operations for OPALS was highly dependent on bi-directional line of sight between the flight system on the ISS and the ground system, requiring pointing accuracy of 300 μradians to receive sufficient power at the ground station. OPALS used a ground beacon to achieve this pointing performance. The ground system used orbital predictions of the ISS to emit the $976\,\mathrm{nm}$ beacon directed at the OPALS flight system. The flight system used a set of blind pointing predictions to search for the ground beacon and achieve a coarse lock. Once the ground beacon was coarsely acquired on the flight system CCD, a PID controller steered the centroid of the beam to the center of the CCD for fine acquisition. The transmit and receive paths on OPALS are co-boresighted, meaning a fine acquisition of the ground beacon also means find pointing of the transmit beam [46].

OPALS used intensity modulation (OOK) to transmit information. Choosing a modest data rate of 50 Mbps allowed for a binary constellation to be used, and a high photon flux of 10,000 photons per bit allowed for the use of a linear-mode avalanche photodetector (APD). Both of these design decisions limit the complexity of the transmitter and receiver and enabled the use of existing COTS components. OPALS uses a (255,233) Reed-Solomon error correcting code. With the link designed to achieve an uncoded bit error rate of $< 10^{-4}$, the coded information could be recovered essentially error free. [7]

E. LLCD - Lunar Laser Communications Demonstration

The Lunar Laser Communications Demonstration was the first attempt at FSO communications from a lunar orbiting spacecraft to a ground based receiver. The LLCD consists of the Lunar Laser Space Terminal (LLST) that was hosted on

the LADEE spacecraft and the Lunar Laser Ground Terminal (LLGT), a mobile terminal that was stationed in White Sands, NM for the demonstration [36]. The NASA Jet Propulsion Laboratory (JPL) OCTL telescope at Table Mountain, California, and the European Space Agency's OGS telescope in Tenerife, Spain were also used as alternative ground terminals. These additional ground terminals were existing telescopes that were retrofitted with optics and electronics to support the LLCD and provided some geographic diversity to make the demonstration, which was limited to the commissioning phase of the LADEE mission, more robust to weather events.

Pointing requirements for the optical link were achieved by using a ground beacon. Similar to OPALS, a-priori information about LADEE's location and attitude were used to initially point the ground beacon at the LLST and vice versa. The LLST would use attitude knowledge from LADEE's star tracker to make it's best effort at pointing toward the ground station. Scanning patterns could be used if the ground beacon was not immediately acquired, although in practice LADEE's attitude knowledge was good enough that this was never required [37]. The LLCD ground beacon differs from the ground beacon used for OPALS in two ways. First, the ground beacon used multiple distinct beams for spatial diversity that were incoherently combined at the LLST and used for tracking. Multiple uplink beams were shown to, both in simulation and experimental data from the LLCD, reduce the scintillation index as received at the LLST [39]. Second, the wavelength of the ground beacon was square-wave modulated at 1 KHz to provide background and detector noise immunity [37]. Additionally, due lunar distances, the LLST used a piezo actuator based lookahead function to correct for the relative velocities and light-time between the LLST and the ground terminal.

The LLST used a 16-PPM (pulse position modulation) downlink with a ½-rate serially concatenated turbo code to encode the downlink data. The 16-PPM symbols were interleaved with a 1-second convolutional channel interleaver. The combination of the turbo code and interleaver enabled reliable error free communication for the LLCD. The LLGT used 4-PPM uplink with the same channel coding. The LLCD demonstrated a reliable 40-622 Mbps downlink and 10-20 Mbps uplink [38]. Over 54 links with the LLGT, the LLCD uplinked 118 GB and downlinked 1.6 TB of data in total. [38]

F. LCRD - Laser Communications Relay Demonstration

The LCRD is a successor to the LLCD. Where the LLCD's lifetime was limited to the commissioning phase of the LADEE mission, the LLCD will be a long running mission in geosynchronous orbit dedicated to demonstrating technologies and developing processes that enable high speed near Earth and deep space FSO communications. Currently scheduled to launch on STPSat-6 in 2020, the LCRD will leverage some components already developed and demonstrated in the LLCD. The LCRD will have two optical communication terminals and will demonstrate high rate Earth-GEO communication, real time optical relay from ground to GEO to ground, power efficient PPM modulation suitable for deep space missions, high speed differential phase shift keying (DPSK) modulation for near Earth communications, and performance of network layers and protocols [3].

The two optical modules on the LCRD will have both PPM and DPSK modulator hardware. The PPM modulator is inherited from the LLCD mission and is capable of up to 622 Mbps. The DPSK modulator is being leveraged from a previous Lincoln Labs project [51] and is capable of 72 Mbps to 2.88 Gbps uncoded data rate. The two optical modules are able to operate and point independently of one another, and are linked together by high speed electronics to operate as a bent pipe relay [52]. Furthermore, the LCRD contains a high bandwidth Ka-band RF module that supports up to 64 Mbps uplink 622 Mbps downlink [53]. Having both high speed RF and optical trunklines, the LCRD is to act as a proving ground for technologies to be used on the Next Generation Tracking and Data Relay Satellites, and will act as a bonafide relay satellite after its technology demonstrations are complete.

Two ground stations are currently planned to be used with the LCRD: the OCTL facility at Table Mountain, CA, and an optical ground station in Hawaii. The same concept for pointing that is seen in OPALS and the LLCD is used, and the ground stations emit a beacon that the LCRD locks onto. Additionally, LEO optical communication modules compatible with the LCRD are planned to be deployed to the ISS, and the LCRD will exercise LEO-GEO-Ground relays as well. The LCRD is to be the stepping stone between the current state-of-the-art relay satellites and future relay technology that will support the growing demand for high speed communications [52]

IV. The Pointing Problem

FSO communications requires significantly better pointing than it's RF counterpart due to the narrow beam widths associated with FSO communications. Studies of FSO communication channels often require very narrow beam widths of less than 5 μrad which are sensitive to velocity aberration, propagation time, and refraction effects [54]. Acquisition, tracking, and pointing (ATP) are mechanisms and processes designed to achieve and maintain an FSO link. Broadly speaking, pointing is the act of aiming the transmitter in the direction of the receiver, acquisition is the process of finely aligning the receiver with the transmitted beam, and tracking is the maintenance of pointing and acquisition throughout the duration of the optical link [55]. ATP concepts can be discussed in terms of mechanisms and processes. Mechanisms are the physical devices and technologies that enable both coarse and precision steering of an optical beam, and processes refer to the concepts and operations of these mechanisms that enable successful acquisition, tracking, and pointing. A variety of ATP mechanisms exist. In the context of satellite based FSO communications, gimbal, mirror, and hybrid gimbal-mirror mechanisms for achieving pointing requirements will be discussed. The types of ATP processes used in satellites can be roughly partitioned into two categories: beacon aided, and beaconless pointing. The former is seen employed by near Earth satellites and is the method of pointing used by all of the

surveyed FSO missions. Beaconless pointing is beneficial for deep space FSO downlinks where distance makes direct tracking of an uplink beacon impractical. Literature on beaconless pointing is dominated around star tracker based methods [56]–[60] and thermal Earth imaging [61], [62]. Hybrid pointing methods have also been discussed in literature in the case where a low rate optical uplink is present in the deep space system which requires much less power to realize than a continuous uplink beacon. In these methods, information about the low rate optical uplink is combined with other pointing references to increase the accuracy of the spacecraft attitude estimate [63].

A. Pointing Loss

When discussing pointing accuracy, it is useful to understand the loss associated with a pointing error. When developing a link budget for an optical communications link, the received power is often expressed as a function of the transmitted power multiplied by a series of gain or loss factors representing a variety of geometric and environmental conditions as described in Equations (1) and (2) The part of G related to pointing loss is denoted in (2) as L_p. L_p can be expressed in a variety of ways and will differ depending on the type of beam considered. Generally, L_p is a function of an angular pointing error, θ_e.

The statistical behavior of θ_e can be described mathematically and represents the performance of the utilized pointing mechanisms. For small error angles, θ_e can be expressed as two orthogonal components (θ_x and θ_y) such that $\theta_e = \sqrt{\theta_x^2 + \theta_y^2}$. Considering θ_x and θ_y as independent Gaussian random variables with means η_x and η_y and variances $\sigma_x^2 = \sigma_y^2 = \sigma^2$, the probability density function (PDF) of θ_e is shown in [64] to be

$$p(\theta_e) = \frac{\theta_e}{\sigma^2} \exp\left(-\frac{1}{2\sigma^2}(\theta_e^2 + \eta^2)\right) I_0\left(\frac{\theta_e \eta}{\sigma^2}\right) \tag{4}$$

where σ^2 is a measure of jitter in the pointing mechanism, $\eta = \sqrt{\eta_x^2 + \eta_y^2}$ is a measure of pointing error due to a constant bias in pointing accuracy, and I_0 is the modified Bessel function of order zero. When $\eta = 0$, $p(\theta_e)$ reduces to

$$p(\theta_e) = \frac{\theta_e}{\sigma^2} \exp\left(-\frac{\theta_e^2}{2\sigma^2}\right) \tag{5}$$

and it is seen that $\theta_e \sim \text{Rayleigh}(\sigma^2)$ which has well known density functions.

As of yet, beam propagation and geometry has not been considered, and thus an exact expression for L_p is not known. However, knowing statistics for θ_e allows some inferences to be made about a failure probability without involving the physics of the beam involved. Consider that, by design or estimation, some critical error angle, δ, is known that cannot be exceeded without causing a communication error. If this angle is exceeded, the power level of the received signal will have faded too low for detection. This event is coined a "pointing induced fade" (PIF), and the probability of a PIF can be determined by the expressions above if the statistical parameters of the pointing mechanism are known [65].

$$\text{PIF} = \mathbb{P}(\theta_e \geq \delta) = \int_{\delta}^{\infty} p(\theta_e) d\theta_e \tag{6}$$

Which can be rewritten as

$$\text{PIF} = 1 - \int_{-\infty}^{\delta} p(\theta_e) d\theta_e = 1 - F_{\theta_e}(\delta) \tag{7}$$

where F_{θ_e} is the cumulative distribution function (CDF) of θ_e. In the case where $\eta = 0$, the CDF of the Rayleigh distribution has a well known analytic expression and the PIF probability is

$$\text{PIF} = \exp\left(\frac{-\delta^2}{2\sigma^2}\right) \tag{8}$$

This simplified result can be used to drive basic requirements for pointing without having developed extreme detail about the system. For example, considering the zero bias case, interesting constraints can be revealed by rearranging (8) to

$$\frac{\delta^2}{\sigma^2} = -2\ln(\text{PIF})$$

In this case, the pointing variance must be $-2\ln(\text{PIF})$ times smaller than the square of the critical angle. If we consider $\text{PIF} = 10^{-6}$ to be sufficiently close to zero for the application, then the pointing variance must be 27.6 times smaller than the square of the critical angle. If this hypothetical system were to require μrad pointing, then it must have pointing variance less than 35 femto radians to achieve a PIF of 10^{-6}. It is clear from this simple example that platform vibrations that cause jitter in optical steering can have negative effects on pointing induced fading, even at small values.

Analytic expressions for L_p can be difficult to determine when considering statistical behavior of θ_e. For link budgets it's often desirable to have a long-run average pointing loss factor, $E(L_p(\theta_e))$, which can involve integrals with no closed form solution. Instantaneous expressions for L_p can be determined by considering gaussian beam geometry with various simplifications such as ignoring extra transverse modes, assuming no obscuration loss at the transmitter, and/or assuming uniform plane-wave illumination [9], [66], [67]. A beam with a Gaussian profile is the simplest beam profile to analyze, and considers only the lowest order transverse mode (known as TEM_{00}) propagating along the beam axis. This mode is often the most desirable, as it propagates with the least divergence. TEM_{00} has a symmetric intensity profile perpendicular to the beam axis that is described by a Gaussian function [68, ch. 5]

$$I(r, z) = A_0 e^{-\frac{2r^2}{w_z^2}} \tag{9}$$

where r is the perpendicular distance from the beam axis, z is the distance along the beam axis, A_0 is the intensity on the beam axis at distance z, and w_z is the beam waist. The beam waist is defined as the distance perpendicular to the beam axis where the intensity has fallen by $1/e^2$ of A_0. The beam waist is a function of the distance along the beam axis, z, and can determined by

$$w(z) = w_0 \sqrt{1 + \left(\frac{\lambda z}{\pi w_0^2}\right)} \tag{10}$$

where w_0 is the minimum beam waist, which usually occurs halfway between the laser mirrors [68]. The minimum beam waist can also be expressed in terms of the beam divergence angle, Θ, which is a common design parameter for FSO systems by

$$\Theta = \frac{2\lambda}{\pi w_0} \tag{11}$$

with λ being the wavelength of the beam. This expression is valid at distances sufficiently far from the optics.

Of interest, now, is the total power received over some receiver area, $\mathcal{A}$, that's a distance, z, from the transmitter. To also capture pointing error, the beam center is considered to be some distance, k, from the center of the receive aperture with the receiver coordinate system centered on the receiver aperture. The receiver area is a circle of radius a (see Figure 2 in [67]). Because of the symmetry of the Gaussian beam profile, the beam can be considered to be offset from the center of the receive aperture in only one axis without loss of generality, which simplifies the problem. If the total power of the beam at distance z is set to unity, the intensity can be integrated over the receiver area to determine the fraction of power received due to both geometric path loss and pointing error. The value of A_0 for unity power can be determined by integrating over a circle of infinite radius and setting the result equal to unity.

$$1 = \int_0^{2\pi} \int_0^{\infty} rI(r;z)drd\theta \tag{12}$$

Solving the integral for A_0 yields

$$A_0 = \frac{2}{\pi w_z^2} \tag{13}$$

The normalized intensity distribution will be denoted

$$\hat{I}(r;z) = \frac{2}{\pi w_z^2} e^{-2\frac{r^2}{w_z^2}} \tag{14}$$

Now, the fraction of received power due to both geometric path loss and pointing error can be written as [67]

$$L_{sp} = \int_{\mathcal{A}} \hat{I}(r-k;z)d\mathcal{A} \tag{15}$$

where L_{sp} indicates the loss factor due to both path loss and pointing loss. For a receiver aperture with radius a, an exact expression for L_{sp} is

$$L_{sp}(k;z) = \int_{-a}^{a} \int_{-\sqrt{a^2-x^2}}^{\sqrt{a^2-x^2}} \frac{2}{\pi w_z^2} e^{-2\frac{(x-k)^2+y^2}{w_z^2}} dydx \tag{16}$$

Note the distance the center of the beam is displaced in the receiver plane is $k = z\tan\theta_e \approx z\theta_e$ when θ_e is small. This expression can be solved numerically. [67] presents a Gaussian form approximation to this integral by instead approximating the receive aperture as a square of the same area which is valid when $w_z \gg a$. This condition is certainly true at the distances involved in communicating from low Earth orbit and beyond. [67] further presents the PDF for this approximation of L_{sp} when k has the same Rayleigh distribution as θ_e, which is valid for small values of θ_e. [69] expands on this PDF and discusses joint statistics including atmospheric scatter that is coupled to the line-of-site component of the propagating beam.

In the above description it was easier to include geometric path loss in addition to pointing loss since both effects are captured by integrating the beam intensity over an area some distance from the transmitter. Other approximations for the instantaneous loss due to pointing exist that don't also include the geometric path loss. While the previously presented loss calculations are complete with probability functions and are useful in channel models, these other approximations for the loss associated with an error angle are better for quick calculations and understanding of the system at hand. Assuming no obscuration at the transmitter and uniform plane-wave illumination, an approximation for L_p is [64], [66]

$$L_p(\theta_e) \approx 4\left[\frac{J_1(\pi D\theta_e/\lambda)}{\pi D\theta_e/\lambda}\right]^2 \tag{17}$$

where J_1 is the Bessel function of order one and D is the diameter of the receiving aperture. [9], [66] also discuss alternate formulations of the above approximation that include transmitter obscuration and other transmitter defects, and further discuss approximations for $E(L_p)$ with the Rayleigh distributed θ_e. Another approximation for L_p is presented in [70]

$$L_p(\theta_e) \approx \exp(-G_t\theta_e^2) \tag{18}$$

where G_t is the transmitter gain.

B. Mechanisms

FSO systems that employ a narrow beam depend heavily on ATP mechanisms for the successful establishment of the optical link. In satellite FSO communications, gimbal based and gimbal-mirror based mechanisms are frequently seen, as many of the surveyed missions use these technologies for pointing. Most pointing mechanisms are mechanical in nature and move physically to steer the beam. There also exist non-mechanical beam steering technologies that have been the subject of research known as electro-optic beam steering. Pointing systems can also include mechanisms to focus a beam or correct wavefront distortions such as adaptive optics, which are discussed in Section V-A. This section will discuss high level categories of pointing mechanisms and their relation to spacecraft and the realization of FSO communications in space. An excellent and more complete survey of FSO ATP mechanisms can be found in [55].

In space based FSO, optical heads require the ability to point over a wide range of angular positions depending on the pointing ability of the host spacecraft. An optical terminal can use a gimbal which employs a rotary mechanism controlled by motors to accomplish this. Gimbals are frequently used for coarse pointing in spacecraft [71]–[73] and, in some cases, the spacecraft body itself can behave as a gimbal when the optical terminal has no supplementary steering capabilities. This scenario was seen for the VSOTA instrument which was rigidly fixed to the host spacecraft (Section III-C). The angular pointing resolution for readily available gimbal components is on the order of μ radians [55]. To achieve this resolution, motors are coupled with reduction gear boxes. A special

type of gear box, often referred to by the trademarked name HarmonicDrive [74], that is similar to a planetary gear box is popular in space applications for its set of highly favorable characteristics that set it apart from traditional gear boxes. Primarily, traditional gearboxes suffer from a backlash effect, wherein there is excess clearance between gear teeth that results in some play in the gears. When backlash is present, there is loss of contact between teeth and the assembly can move when the motor is not in motion or when the motor changes direction [75]. In precision pointing, this is a highly undesirable effect, as backlash will result in a degradation in angular resolution. Harmonic drives, on the other hand, tout a high load capacity, zero backlash, and high torsional stiffness in a single stage co-axial shaft [76], [77]. Controllers that use harmonic drives have been demonstrated to have resolutions that are an order of magnitude better than conventional methods [78]. Further, high torsional stiffness eliminates the needs for locks to hold the gimbal in place during launch, reducing design complexity [79]. Gimbal mechanisms are, however, heavy by nature. They involve more components and dedicated motors and structures. Using an optical gimbal implies increased weight, which the host spacecraft will need to support.

In addition to gimbal mechanisms, mirror mechanisms are commonly seen in FSO communications systems for their ability to steer to sub-μrad levels [55]. Fast steering mirrors (FSMs) are small, light weight mirrors that can make fine adjustments in orientation to reflect incident light onto a receiver. As a result, gimbal-mirror hybrid mechanisms are useful for space applications and are seen implemented in several experimental missions including OPALS, LLCD, and the future LCRD. In these devices, a wide field of view gimbal mechanism is used for coarse steering of the beam onto an FSM, and the FSM further and more precisely steers the beam onto the receiving sensors. FSMs generally fall into three categories based on the type of actuator used to power them: voice coil actuators (VCA) [80], piezoelectric actuators (PZT), and micro-electromechanical systems (MEMS) [55]. VCA FSMs typically have a wider range of available motion, but have lower resonant frequencies that limit their response times. Alternatively, PZT driven FSMs have high resonant frequencies (up to KHz), but only have a few microns of available displacement [81]. PZT actuators also require high voltages to actuate (hundreds of volts), and may exhibit nonlinearities that require complex controllers to drive [55]. Literature discussing the control of PZT actuators can be found in [82]. In [81], a PZT actuator is described that has three PZT pistons, each of which is attached to a small mirror in a triangular format. The three pistons can be actuated to move up a few microns, and the coordination of the three can result in fast and accurate tip/tilt motions of the mirror. MEMs deformable mirrors are small mirrors that are capable of deforming the mirror surface by electronic actuation. These small deformable mirrors can be fabricated in arrays resulting in a 2D deformable mirror [55], similar to multi-section mirrors with individual actuators [83]. MEMs mirrors are most often used for wavefront correction in adaptive optics, but can also be used for tip/tilt action [55].

In space applications, it's desirable to reduce the amount of moving parts on a spacecraft or, if possible, entirely eliminate them. Moving parts apply torques on the spacecraft body and will induce rotations that will interfere with attitude control systems. The Voyager spacecraft, as an example, contained tape drives for data storage, and Voyager operations required detailed understanding of the momentum induced by the tape drives and methods for cancelling it [84]. If an optical terminal requires moving parts, the host spacecraft will need to be able to compensate for it which increases the complexity of the mission. A budding technology in optical communications is non-mechanical electro-optic beam steering. Non-mechanical beam steering utilizes zero moving parts and modifies the beam path by making changes to the wavefront by creating optical path delays or phase differences [85]. Low SWaP, wide field of view (50° by 15°) non mechanical beam steering has been demonstrated in [86].

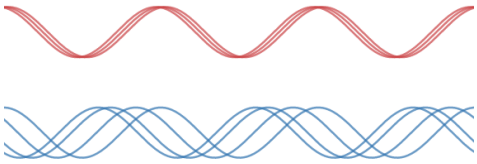

Fig. 3. Coherent light (top, red), and non-coherent light (bottom, blue)

V. Communication

Discussion of communication necessitates a discussion on *how* the communication occurs. In optical communications, information is encoded by varying properties of light. For example, information can be transmitted by varying the intensity of a laser beam. The act of varying the physical properties of light to encode information is called modulation. On the other hand, the act of decoding the information stored in the light by observing changes in its physical properties is called demodulation. Similar to RF communications, information can be coded on the intensity, frequency, and phase of light. Light, however, differs from radio waves in a number of ways, and detection and demodulation of light has unique nuances. This section will discuss current and common methods for detecting light in FSO communications, as well as popular modulation schemes for space based FSO communications and the motivations behind choosing one particular scheme over another.

A. Receivers

Methods for detection of light can be broken into two categories: coherent and non-coherent. Coherence, in light, refers to how much various parts of a beam are in phase [68], where a "beam" consists of the propagation of many individual photons. In a coherent beam, all photons are "in step", and change in phase at the same time. Conversely, and incoherent beam would exhibit random change in phase between photons. Figure 3 shows an illustration of coherent and non-coherent light. In this figure, each wave represents the propagation of

an individual photon. In the coherent case (shown in red), all of the photons are "in step". In the incoherent case (shown in blue), the photons are "out of step", and change phases at different times. Encoding of information on the phase of light requires both a coherent beam and the ability to detect the coherent beam on the receiving end. In coherent systems, amplitude, frequency, phase, and/or polarization modulations can be used. In non-coherent systems, information can be conveyed only by modification of the intensity of the beam.

In either case, photodetectors are used to detect incident light. There are many types of photodetectors [68, ch. 6], the commonly utilized type in FSO communications being photodiodes. Photodiodes are PN junction diodes made from materials that are sensitive to light. The specific materials used are dependent on the wavelengths of light that the diode needs to be sensitive to. These diodes are reverse biased (a positive voltage is applied to the N-type region), and incident light causes an increase in current through the diode. A particular type of photodiode, the avalanche photodiode (APD) is a variant that, by construction, allows for very high reverse bias voltages without breakdown. The higher reverse bias level allows APDs to increase a received signal hundreds of times more than a regular photodiode. Photodiodes have a wavelength dependent responsivity, R, which is a measure of how much the current through the diode will increase given a certain amount of light incident on the photodiode. The responsivity has units of amps per watt, and is also sometimes referred to as "photosensitivity" [68]. Also associated with photodiodes is a measure of quantum efficiency or quantum yield, which is the percentage of incident photons that cause the desired effect of increased current through the diode. Quantum efficiencies of APDs are around 80% to 90% on the high end [87].

APDs can typically be operated in two modes: linear or Geiger [88]. In linear mode operation, the APD is reverse biased below its breakdown voltage, and the current induced is linearly proportional to the intensity of light incident on the detector. This is the least complex way to operate an APD, as linear responses in electronics are fairly easy to work with. In this mode, there is some current that passes through the diode even in the total absence of light called the dark current. Traditionally, APDs operated in linear mode have not been sensitive enough to detect single photons, as the increase in current due to one photon is not measurably different from the dark current. As a result, modulation schemes with high photon flux are seen used with linear mode APDs as was the case for the OPALS mission. There are, however, some APDs meant to do photon counting in linear mode [89].

APDs operated in Geiger mode are meant for single photon counting. In this mode, APDs are sometimes referred to as single photon avalanche diodes (SPADs). In Geiger mode, APDs are reversed biased slightly above their breakdown voltage. When biased above the breakdown voltage, the current induced by incident light completely saturates at any level of received light [88]. As a result, a single incident photon causes a large rush of current. The current will then remain saturated until the electric field over the diode is reduced slightly to below the breakdown voltage. This quench-and-reset operation has to occur for every incident photon, and takes a certain amount of time to complete, limiting the rate at which photons can be counted. Geiger mode operation is an all or nothing situation. Received light results in a predetermined current spike regardless of the intensity of the incident light. Similar to the dark current present in linear mode operation, a dark count is associated with Geiger mode operation. Ideally, the current rush occurs only as a result of an incident photon. Realistically, the charge carrier that results in current saturation can also be generated thermally, which represents a characteristic noise of the detector [90]. The dark count is the frequency at which the SPAD is triggered in the complete absence of light, and limits the sensitivity of SPADs. The dark count is a temperature dependent phenomenon, and can be on the order of kilohertz. Cooling the photodiode to reduce thermal noise can reduce the dark count. For every 8°C temperature reduction, the dark count will reduce approximately by half [87].

There are benefits and drawbacks to both linear and Geiger mode APD operations. The dark current can be thresholded out in linear mode operation, but greater photon flux is required to produce measurable photocurrent. Geiger mode APDs can detect single photons, but will also have a non-zero dark count. Since all events in Geiger mode result in the same current rush, dark counts cannot be thresholded out like the dark current can in linear mode. APDs are not the only type of photodiodes that can be used for photon counting or optical communications. For the LLCD, one of the optical ground stations used a photon counting receiver based on arrays of superconducting nanowire single photon detectors (SNSPDs) which operate at cryogenic temperatures ($\sim$3K) [91]. SNSPDs are capable of achieving an extremely low dark count rate, down to 0.01 Hz [92]–[94].

The photodetector technologies discussed are capable of detecting light intensities. In real FSO receivers, some optical pre-processing may have to be done before the light reaches the photodetector as the photodetectors only sense the presence of light. This can come in the form of correcting deficiencies created by propagation through a medium or optical mixing required for demodulating schemes other than intensity modulation. For reception of beams that propagate through the atmosphere, adaptive optics (AO) are popular for correcting wavefront distortions that are induced by atmospheric turbulence. This is especially true for coherent systems, where atmospheric wavefront distortions (phase delays) have a negative effect on mixing the received signal with a local oscillator (LO) [95]. AO refers to the use of deformable mirrors to correct wavefront aberrations caused by atmospheric turbulence. Wavefront aberrations and atmospheric conditions are measured by sensors in real time at the receiver, and the deformable mirror is actuated to compensate for the measured or estimated disturbances [96]. The deformable mirror corrects the wavefront phase by forming a conjugate of the wavefront shape. The deformable mirror is, of course, composed of discrete actuatable mirrors, and the formation of the conjugate shape will suffer from some quantization errors [97]. A typical measure of the effectiveness of an AO system is the Strehl ratio, which is the ratio of the average intensity at a point at the receiver and the maximum intensity if the wavefront were perfectly flat [97]. A Strehl ratio of 0 is the worst possible deformation in the wavefront,

and a Strehl ratio of 1 corresponds to the best possible case of a flat wavefront. Another performance metric of AO systems is the coupling efficiency, which is the percentage of received light that is coupled to the detector. JPL's OCTL optical ground station achieved a Strehl ratio of approximately 0.6 during an AO corrected OPALS downlink [98], and can achieve a coupling efficiency of around 0.5-0.75 under various atmospheric conditions [99].

B. Modulation and Detection

In satellite FSO communications, three modulation schemes have been identified as good candidates for near Earth and deep space missions: on-off keying (OOK), pulse position modulation (PPM), and differential phase shift keying (DPSK). Each modulation scheme has costs and benefits, and the selection of modulation represents a trade off between complexity of implementation, power requirements, and bandwidth requirements. In RF communications, a wide variety of modulation schemes can be realized with relatively simple hardware. Today, RF modulation can be done entirely in software with the advent of software defined radio (SDR) where waveforms can be generate digitally. Optical communications pose some different challenges, and the types of modulations are limited by what can be realistically implemented in hardware, making the complexity associated with a modulation scheme far more of an impactful metric. On the other hand, bandwidth utilization in RF communications is much more of a concern as the available spectrum has become increasingly congested. The part of the electromagnetic spectrum utilized by optical communications is orders of magnitude higher in frequency than the band utilized by RF communications, opening up a huge amount of bandwidth. Additionally, FSO communications are inherently very directional which virtually eliminates the problem of interfering with neighboring satellites. As a result, bandwidth utilization is not a particular concern in optical communications and the driving factors in the modulation trade space are reduction of the power required for successful exchange of information and reduction of implementation complexity. Following, the three previously mentioned modulation schemes will be defined and discussed in terms of their costs and benefits as they pertain to optical communications. Additionally, detection and demodulation techniques are discussed. For further reading, a survey on FSO communications from a communications theory perspective that presents a wider view of optical modulation can be found in [5].

M-ary communications is a concept prevalent in communications theory to describe modulation schemes [8]. An M-ary modulation scheme is made up of M unique signals that each represent a unique combination of $\log_2 M$ bits. For example, when $M = 4$, two bits are transmitted for each signal that is transmitted. Each unique signal, also called a symbol, is defined for one symbol period (or slot) spanning T seconds. To communicate long sequences of bits, symbols are transmitted one after the other until the entire message is transmitted. This is a generic way to talk about many different modulation schemes. Often, a modulation scheme is prefixed with a number, such as "2-PSK", which indicates that the modulation type is phase shift keying with $M = 2$ unique symbols in the signal set. Figure 4 shows example signal sets for OOK, PPM, and PSK.

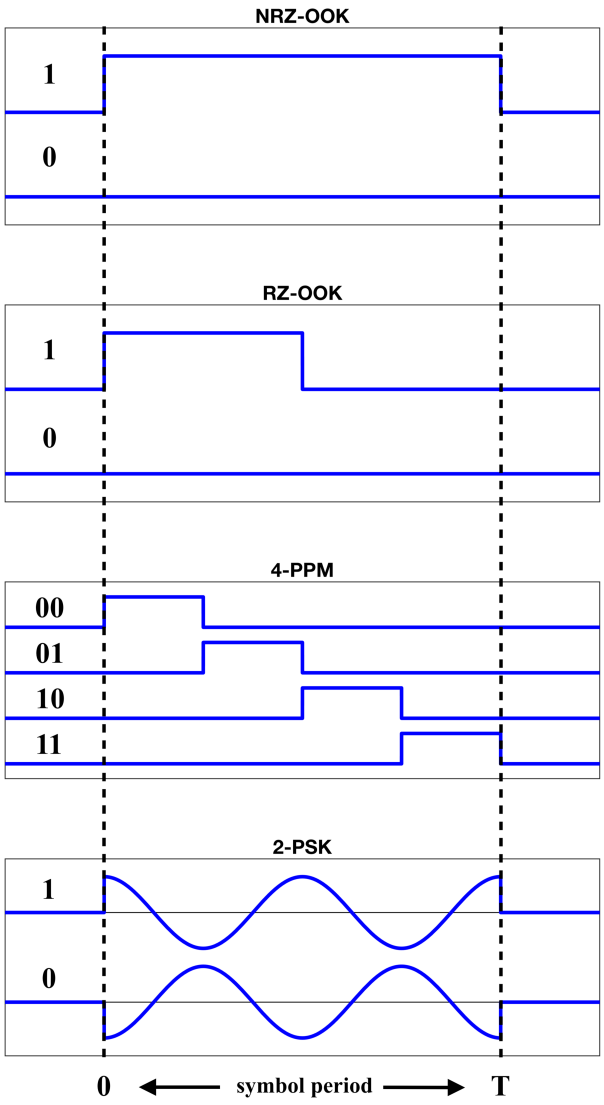

Fig. 4. Waveforms of OOK, PPM, and PSK modulation schemes. For each symbol period, a different waveform is transmitted to represent a bit or group of bits.

OOK is the simplest modulation scheme that can be implemented in optical communications. In this scheme, $M = 2$, and 1 bit is transmitted per symbol. A 1 is transmitted by keying the laser on, and a 0 is transmitted by turning the laser off. This modulation scheme can also be referred to as 2-pulse amplitude modulation (2-PAM). Two variants of OOK are commonly referred to: return-to-zero (RZ-OOK), and non-return-to-zero (NRZ-OOK) [100]. In RZ-OOK, the signal is guaranteed to be returned to the zero level after every bit is transmitted. In NRZ-OOK, the opposite is the case, and two consecutively transmitted ones will leave the laser keyed on for two symbol periods. The difference between the two is shown in Figure 4. In optical communications, OOK is very simple to implement and detect. Some considerations

will need to be made if propagating through the atmosphere such as dynamic thresholding and/or automatic gain control to compensate for atmospheric fading. Despite being the least complex to implement, OOK is not very power efficient and requires a relatively large signal to noise ratio when compared to other modulation schemes [5]. This modulation scheme, along with other intensity modulations, will suffer from reduced sensitivity at low Sun angles where there is increase background noise.

PPM is a favored modulation scheme in FSO communications for both it's simplicity to implement and high power efficiency. The PPM modulation scheme encodes information by the placement (position) of a pulse in the symbol period. In Figure 4, an example 4-PPM symbol set is shown. Here, $M = 4$, and there are four unique symbols in the set. Each symbol is a square pulse that occurs at a different part of the symbol slot. In this case, the slot is divided into four equal sections, and each symbol contains a pulse that occupies one of the sections. Since there are 4 symbols in the set, each transmitted symbol carries two bits of information. Here, the first symbol encodes bits 00, the second encodes bits 01, and so on. The mapping of bits to symbols is arbitrary in this case, as PPM is an orthogonal modulation and no bit mapping has any advantage over another [8]. This is true for all orthogonal modulation schemes, but not not in general. M-PPM modulations can be near capacity-achieving, meaning they can approach the theoretical quantum limit in power needed to convey a message. The power efficiency of PPM has long been identified [101]. The PPM modulation and photon counting receiver for the LLCD required only nano watts of power at the receiver, with sensitivities approaching a few photons/bit [102]. PPM is an intensity modulation, like OOK. As a result, the complexity of PPM implementation is not particularly extreme. Due to the near capacity power efficiencies that can be achieved and the limited complexity of implementation, PPM is ideal for long haul deep space communications. However, high sensitivity photon counting receivers can be difficult to put on spacecraft, which limits the uplink capability for PPM. This is reflected in the surveyed missions, where PPM uplinks are operated at significantly lower data rates than PPM downlinks.

Intensity modulations have been favored in early FSO implementations and experiments due to their simplicity. Other modulation schemes that aren't intensity dependent are beginning to make their way into the mix as our ability to implement optical technologies gets more sophisticated, power efficient, and miniaturized. PSK is implemented by varying the phase of the transmitted signal. In Figure 4, 2-PSK, also called binary PSK (BPSK), is pictured, where a sine wave is the symbol corresponding to bit 1 and a sine wave shifted by 180° in phase represents bit 0. M is not limited to 2 in PSK modulations. 4-PSK and upwards can be frequently found in RF communications. A special variant of PSK, differential PSK (DPSK) has been explored for FSO communications. Differential PSK is a type of 2-PSK where the phase difference between two symbols encodes the bit instead of the absolute phase of the symbol. This is a highly beneficial trait for receiving this type of optical modulation as it removes the need for mixing with a matched local optical oscillator. Such a local oscillator would need to be phase locked to the transmitter oscillator, a process which can take tens of seconds and be problematic [51]. Due to DPSK not being an intensity modulation, DPSK receivers will be less sensitive to fluctuations in received power. In fact, DPSK provides good immunity against solar background noise [6]. DPSK modulation can be implemented using a Mach-Zehnder modulator, and DPSK demodulation can be implemented by using a Mach-Zehnder delay interferometer [51]. Although more complex than intensity modulations, these technologies are becoming more reasonable to put in power starved areas like space. Being able to achieve data rates on the order of Gbps, DPSK is a good modulation choice for near Earth communications where the complexity in (de)modulation hardware can be afforded [103]. Relay satellites, in particular, are a good place for DPSK modulation as the reception hardware can be reasonably put on satellites allowing for high data rates in both directions.

Optical detection techniques have their own set of nomenclature, though many of the concepts are similar to or stem directly from RF communications. There are two classes of detection techniques that encompass the discussed modulation types: non-coherent (PAM, PPM) and coherent detection (DPSK, PSK, or any other) [104]. As previously discussed, optical coherence refers to the consistency of phase amongst all photons that make up a beam. Accordingly, non-coherent detection techniques cannot recover phase information, and coherent techniques can. First, coherent detection is discussed, as all of the mentioned modulation schemes could theoretically be coherently detected. Coherent detection stems from the RF concept of downconversion. Here, the inbound optical signal is mixed with a LO of a known frequency in an optical coupler resulting in a lower frequency signal which, in the best case, is baseband. The down-converted optical signal is turned into an electrical signal via linear mode photodiodes and further processed electrically. If the LO is locked exactly to the frequency of the received signal, it is called homodyne detection [105]. Homodyne detection requires an accurate phase locked loop, which is expensive to realize [5]. At the same time, homodyne detected BPSK provides full immunity against sunlight [106]. If the LO has a different frequency than the received signal, however small, it is called heterodyne detection. A special case is DPSK, which can be considered to be self-homodyne [107] in that it can be mixed with itself via a delay interferometer upon reception and then captured via photodiodes. In this sense, the self-homodyne signal also carries the LO that it's mixed with and no expensive phase or frequency locking of an LO is required at the receiver. All optical signals can be coherently detected through either a heterodyne or homodyne implementation, but modulation schemes that encode information on frequency or phase must be coherently detected. Non-coherent detection techniques refers to a optical detection that only captures the level of energy at the receiver, and is also sometimes referred to as direct detection. Direct detection is accomplished with photodiodes, either linear or photon counting, as discussed in the previous section. Any intensity modulated signal (OOK,

PPM) can be directly detected. Direct detection requires no optical pre-processing and, as a result, receivers can be more simple and less costly to realize. This is not always the case, however, for expensive or power hungry single photon counting diodes.

VI. Summary and Discussion

FSO communications have the potential to fill future needs for faster data transfer at greater distances. It is strongly believed that FSO communications will play a big role in next generation communication relay satellites and future deep space missions. Opening up more bandwidth for use will enable new types of scientific missions and support new, especially crewed, interplanetary activities. FSO communications have been studied for decades, but the technologies involved are still in their infancies and are only recently getting to a readiness level where they can be fielded for actual use. The LCRD will demonstrate this, tentatively in 2020, by acting as a full fledged optical/RF relay satellite. FSO communications is not without its challenges, however, and the trade space is vast and complex. Design choices for modulation and detection trade between implementation complexity and SWaP requirements. FSO communication through the atmosphere presents a host of challenges such as optical ground station placement to minimize cloud coverage and maximize link availability. Optical ground station telescopes today utilize extraordinary state-of-the-art adaptive optics systems to correct for wavefront distortions caused by atmospheric turbulence. Pointing requirements for optical communications are much more strict than those required for RF communications. All of the FSO demonstrations surveyed in this paper utilize beacon aided pointing, wherein the transmitter uses a reference beacon supplied by the receiver for fine pointing and tracking. Missions that venture further will likely need to explore beaconless pointing methods and alternative ways to achieve the same pointing accuracy. A wide variety of mechanisms are available to build pointing devices, and acquisition, tracking, and pointing represents an entire discipline by itself. Optical modulation techniques share many similarities to RF modulation techniques, but implementations can differ drastically. The optical modulations available for use is limited both by the existence of the technology to implement them and the practicality of hosting that technology on a spacecraft. This paper has discussed these topics in FSO communications at a high level and is by no means comprehensive. The field of FSO communications is vast, and current research and technology demonstrations are moving forward at exciting paces. It is hoped that the concepts and research presented in this paper motivate further study and efforts in the development of FSO technologies that will power next generation communications.

References

[1] A. G. Alkholidi and K. S. Altowij, "Free Space Optical Communications — Theory and Practices," in *Contemporary Issues in Wireless Communications*, M. Khatib, Ed. InTech. [Online]. Available: http://www.intechopen.com/books/contemporary-issues-in-wireless-communications/free-space-optical-communications-theory-and-practices

[2] L. Deutsch, "Meeting the communications challenges of NASA's future deep space missions," accepted: 2019-11-06T17:55:46Z. [Online]. Available: https://trs.jpl.nasa.gov/handle/2014/46998

[3] B. L. Edwards, D. Israel, K. Wilson, J. Moores, and A. Fletcher, "Overview of the Laser Communications Relay Demonstration Project," p. 18.

[4] "Spectrum occupancy measurements and evaluation," international Telecommunication Union. ITU-R SM.2256-1.

[5] M. A. Khalighi and M. Uysal, "Survey on Free Space Optical Communication: A Communication Theory Perspective," vol. 16, no. 4. [Online]. Available: https://ieeexplore.ieee.org/document/6844864/

[6] H. Kaushal and G. Kaddoum, "Optical Communication in Space: Challenges and Mitigation Techniques," vol. 19, no. 1, pp. 57–96, Firstquarter 2017.

[7] B. V. Oaida, W. Wu, B. I. Erkmen, A. Biswas, K. S. Andrews, M. Kokorowski, and M. Wilkerson, "Optical link design and validation testing of the Optical Payload for Lasercomm Science (OPALS) system," H. Hemmati and D. M. Boroson, Eds., p. 89710U. [Online]. Available: http://proceedings.spiedigitallibrary.org/proceeding.aspx?doi=10.1117/12.2045351

[8] J. G. Proakis and M. Salehi, *Digital Communications*, oCLC: 1097253849.

[9] W. K. Marshall and B. D. Burk, "Received optical power calculations for optical communications link performance analysis." [Online]. Available: http://adsabs.harvard.edu/abs/1986tdar.nasa…32M

[10] B. J. Geldzahler, J. Rush, L. J. Deutsch, and J. I. Statman, "Engineering the Next Generation Deep Space Network," in *2007 IEEE/MTT-S International Microwave Symposium*.

[11] O. Kegege, M. Fuentes, N. Meyer, and A. Sil, "Three-dimensional analysis of Deep Space Network antenna coverage," in *2012 IEEE Aerospace Conference*.

[12] S. Poulenard, M. Ruellan, B. Roy, J. Riédi, F. Parol, and A. Rissons, "High altitude clouds impacts on the design of optical feeder link and optical ground station network for future broadband satellite services," H. Hemmati and D. M. Boroson, Eds. [Online]. Available: http://proceedings.spiedigitallibrary.org/proceeding.aspx?doi=10.1117/12.2038486

[13] G. S. Wojcik, H. L. Szymczak, R. J. Alliss, R. P. Link, M. E. Craddock, and M. L. Mason, "Deep-space to ground laser communications in a cloudy world," D. G. Voelz and J. C. Ricklin, Eds. [Online]. Available: http://proceedings.spiedigitallibrary.org/proceeding.aspx?doi=10.1117/12.615435

[14] S. Poulenard, M. Crosnier, and A. Rissons, "Ground segment design for broadband geostationary satellite with optical feeder link," vol. 7, no. 4, pp. 325–336.

[15] C. Fuchs and F. Moll, "Ground station network optimization for space-to-ground optical communication links," vol. 7, no. 12, pp. 1148–1159.

[16] M. S. Net, I. D. Portillo, E. Crawley, and B. Cameron, "Approximation methods for estimating the availability of optical ground networks," vol. 8, no. 10, pp. 800–812.

[17] N. K. Lyras, C. I. Kourogiorgas, and A. D. Panagopoulos, "Cloud Attenuation Statistics Prediction From Ka-Band to Optical Frequencies: Integrated Liquid Water Content Field Synthesizer," vol. 65, no. 1, pp. 319–328.

[18] N. K. Lyras, C. N. Efrem, C. I. Kourogiorgas, and A. D. Panagopoulos, "Optimum Monthly Based Selection of Ground Stations for Optical Satellite Networks," vol. 22, no. 6, pp. 1192–1195.

[19] N. K. Lyras, C. I. Kourogiorgas, and A. D. Panagopoulos, "Cloud free line of sight prediction modeling for low earth orbit optical satellite networks," in *International Conference on Space Optics — ICSO 2018*, N. Karafolas, Z. Sodnik, and B. Cugny, Eds. SPIE, p. 51. [Online]. Available: https://www.spiedigitallibrary.org/conference-proceedings-of-spie/11180/2535971/Cloud-free-line-of-sight-prediction-modeling-for-low-earth/10.1117/12.2535971.full

[20] NASA Earth Observations (NEO). [Online]. Available: https://neo.sci.gsfc.nasa.gov/

[21] D. M. Boroson, A. Biswas, and B. L. Edwards, "MLCD: Overview of NASA's Mars laser communications demonstration system," in *Free-Space Laser Communication Technologies XVI*, vol. 5338. International Society for Optics and Photonics, pp. 16–28. [Online]. Available: https://www.spiedigitallibrary.org/conference-proceedings-of-spie/5338/0000/MLCD-overview-of-NASAs-Mars-laser-communications-demonstration-system/10.1117/12.543014.short

[22] A. Biswas, D. Boroson, and B. Edwards, "Mars laser communication demonstration: What it would have been," in *Free-Space Laser Communication Technologies XVIII*, vol. 6105. International Society for Optics and Photonics, p. 610502. [Online]. Available:

https://www.spiedigitallibrary.org/conference-proceedings-of-spie/6105/610502/Mars-laser-communication-demonstration-what-it-would-have-been/10.1117/12.669551.short

[23] H. Hemmati, A. Biswas, and I. B. Djordjevic, "Deep-Space Optical Communications: Future Perspectives and Applications," vol. 99, no. 11, pp. 2020–2039.

[24] D. Boroson, C.-C. Chen, and B. Edwards, "Overview of the Mars laser communications demonstration project," in *Digest of the LEOS Summer Topical Meetings, 2005.*, pp. 5–7.

[25] A. Biswas, F. Khatri, and D. Boroson, "Near-Sun free-space optical communications from space," in *2006 IEEE Aerospace Conference*, pp. 9 pp.–.

[26] HORIZONS Web-Interface. [Online]. Available: https://ssd.jpl.nasa.gov/horizons.cgi

[27] M. Jeganathan, M. Toyoshima, K. E. Wilson, J. C. James, G. Xu, and J. R. Lesh, "Data analysis results from the GOLD experiments," G. S. Mecherle, Ed., pp. 70–81. [Online]. Available: http://proceedings.spiedigitallibrary.org/proceeding.aspx?articleid=1028200

[28] M. Toyoshima, K. Araki, Y. Arimoto, M. Toyoda, M. Jeganathan, K. Wilson, and J. R. Lesh, "Reduction of ETS-VI Laser Communication Equipment Optical-Downlink Telemetry Collected During GOLD," p. 9.

[29] K. E. Wilson and J. R. Lesh, "Overview of the Ground-to-Orbit Lasercom Demonstration," p. 8.

[30] K. Wilson, M. Jeganathan, J. R. Lesh, J. James, and G. Xu, "Results From Phase-1 and Phase-2 GOLD Experiments," p. 11.

[31] R. Lange and B. Smutny, "BPSK laser communication terminals to be verified in space," in *IEEE MILCOM 2004. Military Communications Conference, 2004.*, vol. 1, pp. 441–444 Vol. 1.

[32] D. Giggenbach, J. Horwath, and M. Knapek, "Optical data downlinks from Earth observation platforms," in *Free-Space Laser Communication Technologies XXI*, vol. 7199. International Society for Optics and Photonics, p. 719903. [Online]. Available: https://www.spiedigitallibrary.org/conference-proceedings-of-spie/7199/719903/Optical-data-downlinks-from-Earth-observation-platforms/10.1117/12.811152.short

[33] F. Heine, H. Kämpfner, R. Czichy, R. Meyer, and M. Lutzer, "Optical inter-satellite communication operational," in *2010 - MILCOM 2010 MILITARY COMMUNICATIONS CONFERENCE*, pp. 1583–1587.

[34] T. Schwander, R. Lange, H. Kämpfner, and B. Smutny, "LCTSX: First on-orbit verification of a coherent optical link," in *International Conference on Space Optics — ICSO 2004*, vol. 10568. International Society for Optics and Photonics, p. 105682H. [Online]. Available: https://www.spiedigitallibrary.org/conference-proceedings-of-spie/10568/105682H/LCTSX--first-on-orbit-verification-of-a-coherent-optical/10.1117/12.2500115.short

[35] S. Constantine, L. E. Elgin, M. L. Stevens, J. A. Greco, K. Aquino, D. D. Alves, and B. S. Robinson, "Design of a high-speed space modem for the lunar laser communications demonstration," H. Hemmati, Ed., p. 792308. [Online]. Available: http://proceedings.spiedigitallibrary.org/proceeding.aspx?doi=10.1117/12.878927

[36] B. S. Robinson, D. M. Boroson, D. A. Burianek, and D. V. Murphy, "The lunar laser communications demonstration," in *2011 International Conference on Space Optical Systems and Applications (ICSOS)*, pp. 54–57.

[37] D. M. Boroson, B. S. Robinson, D. V. Murphy, D. A. Burianek, F. Khatri, J. M. Kovalik, Z. Sodnik, and D. M. Cornwell, "Overview and results of the Lunar Laser Communication Demonstration," H. Hemmati and D. M. Boroson, Eds., p. 89710S. [Online]. Available: http://proceedings.spiedigitallibrary.org/proceeding.aspx?doi=10.1117/12.2045508

[38] B. S. Robinson, D. M. Boroson, D. Burianek, D. Murphy, F. Khatri, A. Biswas, Z. Sodnik, J. Burnside, J. Kansky, and D. M. Cornwell, "The NASA Lunar Laser Communication Demonstration—Successful High-Rate Laser Communications To and From the Moon," in *SpaceOps 2014 Conference*. American Institute of Aeronautics and Astronautics. [Online]. Available: http://arc.aiaa.org/doi/10.2514/6.2014-1685

[39] A. Biswas and S. Piazzolla, "Multi-beam laser beacon propagation over lunar distance: Comparison of predictions and measurements," H. Hemmati and D. M. Boroson, Eds., p. 1009607. [Online]. Available: http://proceedings.spiedigitallibrary.org/proceeding.aspx?doi=10.1117/12.2254976

[40] Y. Koyama, M. Toyoshima, Y. Takayama, H. Takenaka, K. Shiratama, I. Mase, and O. Kawamoto, "SOTA: Small Optical Transponder for micro-satellite," in *2011 International Conference on Space Optical Systems and Applications (ICSOS)*, pp. 97–101.

[41] T. Kuwahara, K. Yoshida, Y. Sakamoto, Y. Tomioka, K. Fukuda, M. Fukuyama, N. Sugimura, H. Kunimori, H. Takenaka, M. Toyoshima, T. Fuse, and T. Kubooka, "Satellite-to-ground optical communication system on Low Earth Orbit micro-satellite RISESAT," in *2012 IEEE/SICE International Symposium on System Integration (SII)*, pp. 939–944.

[42] E. Samain, D.-H. Phung, N. Maurice, D. Albanesse, H. Mariey, M. Aimar, G. Lagarde, N. Vedrenne, M.-T. Velluet, G. Artaud, J.-L. Issler, M. Toyoshima, M. Akioka, D. Kolev, Y. Munemasa, H. Takenaka, and N. Iwakiri, "First free space optical communication in europe between SOTA and MeO optical ground station," in *2015 IEEE International Conference on Space Optical Systems and Applications (ICSOS)*, pp. 1–7.

[43] H. Takenaka, Y. Koyama, M. Akioka, D. Kolev, N. Iwakiri, H. Kunimori, A. Carrasco-Casado, Y. Munemasa, E. Okamoto, and M. Toyoshima, "In-orbit verification of small optical transponder (SOTA): Evaluation of satellite-to-ground laser communication links," H. Hemmati and D. M. Boroson, Eds., p. 973903. [Online]. Available: http://proceedings.spiedigitallibrary.org/proceeding.aspx?doi=10.1117/12.2214461

[44] Y. Munemasa, M. Akioka, Y. Koyama, H. Kunimori, and M. Toyoshima, "On-orbit evaluation of satellite-ground laser communication experiment using small optical transponder (SOTA) equipment –Optical Antenna," in *International Conference on Space Optics — ICSO 2016*, N. Karafolas, B. Cugny, and Z. Sodnik, Eds. SPIE, p. 189. [Online]. Available: https://spiedigitallibrary.org/conference-proceedings-of-spie/10562/2296176/On-orbit-evaluation-of-satellite-ground-laser-communication-experiment-using/10.1117/12.2296176.full

[45] H. Tomio, T. Kuwahara, S. Fujita, Y. Sato, M. Sakal, H. Kunimori, T. Kubooka, H. Takenaka, Y. Saito, and M. Toyoshima, "Assembly and integration of optical downlink terminal VSOTA on microsatellite RISESAT," in *International Conference on Space Optics — ICSO 2018*, N. Karafolas, Z. Sodnik, and B. Cugny, Eds. SPIE, p. 214. [Online]. Available: https://www.spiedigitallibrary.org/conference-proceedings-of-spie/11180/2536134/Assembly-and-integration-of-optical-downlink-terminal-VSOTA-on-microsatellite/10.1117/12.2536134.full

[46] B. V. Oaida, M. J. Abrahamson, R. J. Witoff, J. N. B. Martinez, and D. A. Zayas, "OPALS: An optical communications technology demonstration from the International Space Station," in *2013 IEEE Aerospace Conference*. IEEE, pp. 1–20. [Online]. Available: http://ieeexplore.ieee.org/document/6497167/

[47] M. J. Abrahamson, O. Sindiy, B. Oaida, M. Wilkerson, and M. Kokorowski, "OPALS: Mission System Operations Architecture for an Optical Communications Demonstration on the ISS," in *SpaceOps 2014 Conference*. American Institute of Aeronautics and Astronautics. [Online]. Available: http://arc.aiaa.org/doi/10.2514/6.2014-1627

[48] J. M. Kovalik, M. Wright, W. T. Roberts, and A. Biswasa, "Optical Communications Telescope Laboratory (OCTL) Support of Space to Ground Link Demonstrations," in *SpaceOps 2014 Conference*. American Institute of Aeronautics and Astronautics. [Online]. Available: http://arc.aiaa.org/doi/10.2514/6.2014-1710

[49] M. J. Abrahamson, B. V. Oaida, O. Sindiy, and A. Biswas, "Achieving operational two-way laser acquisition for OPALS payload on the International Space Station," H. Hemmati and D. M. Boroson, Eds., p. 935408. [Online]. Available: http://proceedings.spiedigitallibrary.org/proceeding.aspx?doi=10.1117/12.2182473

[50] O. Sindiy, M. Abrahamson, A. Biswas, M. W. Wright, J. H. Padams, and A. Konyha, "Lessons Learned from Optical Payload for Lasercomm Science (OPALS) Mission Operations," in *AIAA SPACE 2015 Conference and Exposition*. American Institute of Aeronautics and Astronautics. [Online]. Available: http://arc.aiaa.org/doi/10.2514/6.2015-4657

[51] D. Caplan, H. Rao, J. Wang, D. Boroson, J. J. Carney, A. Fletcher, S. Hamilton, R. Kochhar, R. Magliocco, R. Murphy, M. Norvig, B. Robinson, R. Schulein, and N. Spellmeyer, "Ultra-wide-range multi-rate DPSK laser communications," in *CLEO/QELS: 2010 Laser Science to Photonic Applications*, pp. 1–2.

[52] B. L. Edwards, D. J. Israel, A. Caroglanian, and J. Spero, "A Day in the Life of the Laser Communications Relay Demonstration Project," in *SpaceOps 2016 Conference*. American Institute of Aeronautics and Astronautics. [Online]. Available: http://arc.aiaa.org/doi/10.2514/6.2016-2590

[53] D. J. Israel, B. L. Edwards, and J. W. Staren, "Laser Communications Relay Demonstration (LCRD) update and the path towards optical relay operations," in *2017 IEEE Aerospace Conference*, pp. 1–6.

[54] E. B. Moss, "Some aspects of the pointing problem for optical communication in space," vol. 2, no. 5, pp. 698–705. [Online]. Available: https://arc.aiaa.org/doi/10.2514/3.28265

[55] Y. Kaymak, R. Rojas-Cessa, J. Feng, N. Ansari, M. Zhou, and T. Zhang, "A Survey on Acquisition, Tracking, and Pointing Mechanisms for Mobile Free-Space Optical Communications," vol. 20, no. 2, pp. 1104–1123. [Online]. Available: https://ieeexplore.ieee.org/document/8288586/

[56] S. Lee, J. W. Alexander, and G. G. Ortiz, "Submicroradian pointing system design for deep-space optical communications," G. S. Mecherle, Ed., pp. 104–111. [Online]. Available: http://proceedings.spiedigitallibrary.org/proceeding.aspx?articleid=901570

[57] G. G. Ortiz and S. Lee, "Star tracker based ATP system conceptual design and pointing accuracy estimation," G. S. Mecherle, Ed., p. 61050D. [Online]. Available: http://proceedings.spiedigitallibrary.org/proceeding.aspx?doi=10.1117/12.660263

[58] A. J. Swank, E. Aretskin-Hariton, D. K. Le, O. Sands, and A. Wroblewski, "Beaconless Pointing for Deep-Space Optical Communication," in *34th AIAA International Communications Satellite Systems Conference*. American Institute of Aeronautics and Astronautics. [Online]. Available: http://arc.aiaa.org/doi/10.2514/6.2016-5708

[59] E. Aretskin-Hariton, A. Swank, and J. S. Gray, "Beaconless Optical Communication System Constraints," in *AIAA Scitech 2019 Forum*. American Institute of Aeronautics and Astronautics. [Online]. Available: https://arc.aiaa.org/doi/10.2514/6.2019-2130

[60] S. Lee, G. G. Ortiz, and J. W. Alexander, "Star Tracker-Based Acquisition, Tracking, and Pointing Technology for Deep-Space Optical communications," p. 18.

[61] A. Biswas, S. Piazolla, G. Peterson, G. G. Ortiz, and H. Hemmati, "The Long-Wave Infrared Earth Image as a Pointing Reference for Deep-Space Optical Communications," p. 30.

[62] S. Lee, G. G. Ortiz, W. T. Roberts, and J. W. Alexander, "Feasibility Study on Acquisition, Tracking, and Pointing Using Earth Thermal Images for Deep-Space Ka-Band and Optical Communications," p. 19.

[63] J. W. Burnside, D. V. Murphy, F. K. Knight, and F. I. Khatri, "A Hybrid Stabilization Approach for Deep-Space Optical Communications Terminals," vol. 95, no. 10, pp. 2070–2081. [Online]. Available: http://ieeexplore.ieee.org/document/4374101/

[64] V. Vilnrotter, "The effects of pointing errors on the performance of optical communications systems."

[65] A. Biswas and S. Piazzolla, "Deep-Space Optical Communications Downlink Budget from Mars: System Parameters," vol. 154, pp. 1–38. [Online]. Available: http://adsabs.harvard.edu/abs/2003IPNPR.154L...1B

[66] W. K. Marshall, "Transmitter pointing loss calculation for free-space optical communications link analyses," vol. 26, no. 11, pp. 2055_1–2057. [Online]. Available: https://www.osapublishing.org/ao/abstract.cfm?uri=ao-26-11-2055_1

[67] A. A. Farid and S. Hranilovic, "Outage Capacity Optimization for Free-Space Optical Links With Pointing Errors," vol. 25, no. 7, pp. 1702–1710.

[68] C. Roychoudhuri, *Fundamentals of Photonics*. SPIE. [Online]. Available: http://ebooks.spiedigitallibrary.org/book.aspx?doi=10.1117/3.784938

[69] A. Jurado-Navas, J. M. Garrido-Balsells, J. F. Paris, M. Castillo-Vázquez, and A. Puerta-Notario, "Impact of pointing errors on the performance of generalized atmospheric optical channels," vol. 20, no. 11, pp. 12 550–12 562. [Online]. Available: https://www.osapublishing.org/oe/abstract.cfm?uri=oe-20-11-12550

[70] S. Arnon, "Effects of atmospheric turbulence and building sway on optical wireless-communication systems," vol. 28, no. 2, pp. 129–131. [Online]. Available: https://www.osapublishing.org/ol/abstract.cfm?uri=ol-28-2-129

[71] E. D. Miller, M. DeSpenza, I. Gavrilyuk, G. Nelson, B. Erickson, B. Edwards, E. Davis, and T. Truscott, "A prototype coarse pointing mechanism for laser communication," H. Hemmati and D. M. Boroson, Eds., p. 100960S. [Online]. Available: http://proceedings.spiedigitallibrary.org/proceeding.aspx?doi=10.1117/12.2264086

[72] A. Cline, P. Shubert, J. McNally, N. Jacka, and R. Pierson, "Design of a stabilized, compact gimbal for space-based free space optical communications (FSOC)," H. Hemmati and D. M. Boroson, Eds., p. 100960G. [Online]. Available: http://proceedings.spiedigitallibrary.org/proceeding.aspx?doi=10.1117/12.2251656

[73] M. E. Rosheim and G. F. Sauter, "Free-space optical communications system pointer," in *Free-Space Laser Communication Technologies XV*, vol. 4975. International Society for Optics and Photonics, pp. 126–133. [Online]. Available: https://www.spiedigitallibrary.org/conference-proceedings-of-spie/4975/0000/Free-space-optical-communications-system-pointer/10.1117/12.501653.short

[74] Harmonic Drive® High Precision Gear — Harmonic Drive. [Online]. Available: https://www.harmonicdrive.net/

[75] L. Walha, T. Fakhfakh, and M. Haddar, "Backlash Effect on Dynamic Analysis of a Two-Stage Spur Gear System," vol. 6, no. 3, pp. 60–68. [Online]. Available: http://www.ingentaselect.com/rpsv/cgi-bin/cgi?ini=xref&body=linker&reqdoi=10.1361/154770206X107325

[76] B. Routh, "Design aspects of harmonic drive gear and performance improvement of its by problems identification: A review," p. 020016. [Online]. Available: http://aip.scitation.org/doi/abs/10.1063/1.5029592

[77] G. A. Timofeyev, Y. V. Kostikov, A. V. Yaminsky, and Y. O. Podchasov, "Theory and Practice of Harmonic Drive Mechanisms," vol. 468, p. 012010. [Online]. Available: https://iopscience.iop.org/article/10.1088/1757-899X/468/1/012010

[78] S.-w. Le and G.-j. Li, "Study of resolution for harmonic drives controller with friction in precision robotic system," in *2011 Eighth International Conference on Fuzzy Systems and Knowledge Discovery (FSKD)*, vol. 4, pp. 2404–2407.

[79] J. Kovalik, H. Hemmati, and A. Biswas, "10-Gb/s lasercom system for spacecraft," in *Free-Space Laser Communication Technologies XXIV*, vol. 8246. International Society for Optics and Photonics, p. 82460F. [Online]. Available: https://www.spiedigitallibrary.org/conference-proceedings-of-spie/8246/82460F/10-Gbs-lasercom-system-for-spacecraft/10.1117/12.908644.short

[80] X. Feng, Z. Duan, Y. Fu, A. Sun, and D. Zhang, "The technology and application of voice coil actuator," in *2011 Second International Conference on Mechanic Automation and Control Engineering*, pp. 892–895.

[81] C. Wei, C. Sihai, W. Xin, and L. Dong, "A new two-dimensional fast steering mirror based on piezoelectric actuators," in *2014 4th IEEE International Conference on Information Science and Technology*, pp. 308–311.

[82] S. Ibrir, C.-Y. Su, B. S. Ooi, and M. S. Alouini, "Fast and reliable control of steering mirrors with application to free-space communication," in *2017 International Conference on Advanced Mechatronic Systems (ICAMechS)*, pp. 483–488.

[83] R. H. Freeman and J. E. Pearson, "Deformable Mirrors For All Seasons And Reasons," in *Wavefront Distortions in Power Optics*, vol. 0293. International Society for Optics and Photonics, pp. 232–242. [Online]. Available: https://www.spiedigitallibrary.org/conference-proceedings-of-spie/0293/0000/Deformable-Mirrors-For-All-Seasons-And-Reasons/10.1117/12.932345.short

[84] H. MARDERNESS, "Voyager engineering improvements for Uranus encounter," in *Astrodynamics Conference*. American Institute of Aeronautics and Astronautics, _eprint: https://arc.aiaa.org/doi/pdf/10.2514/6.1986-2110. [Online]. Available: https://arc.aiaa.org/doi/abs/10.2514/6.1986-2110

[85] P. F. McManamon and A. Ataei, "Progress and opportunities in the development of nonmechanical beam steering for electro-optical systems," vol. 58, no. 12, p. 120901. [Online]. Available: https://www.spiedigitallibrary.org/journals/Optical-Engineering/volume-58/issue-12/120901/Progress-and-opportunities-in-the-development-of-nonmechanical-beam-steering/10.1117/1.OE.58.12.120901.short

[86] M. Ziemkiewicz, S. R. Davis, S. D. Rommel, D. Gann, B. Luey, J. D. Gamble, and M. Anderson, "Laser-based satellite communication systems stabilized by non-mechanical electro-optic scanners," D. J. Henry, G. J. Gosian, D. A. Lange, D. Linne von Berg, T. J. Walls, and D. L. Young, Eds., p. 982808. [Online]. Available: http://proceedings.spiedigitallibrary.org/proceeding.aspx?doi=10.1117/12.2223269

[87] D. Renker, "Geiger-mode avalanche photodiodes, history, properties and problems," vol. 567, no. 1, pp. 48–56. [Online]. Available: https://linkinghub.elsevier.com/retrieve/pii/S0168900206008680

[88] G. M. Williams and A. S. Huntington, "Probabilistic analysis of linear mode vs. Geiger mode APD FPAs for advanced LADAR enabled interceptors," in *Spaceborne Sensors III*, vol. 6220. International Society for Optics and Photonics, p. 622008. [Online]. Available: https://www.spiedigitallibrary.org/conference-proceedings-of-spie/6220/622008/Probabilistic-analysis-of-linear-mode-vs-Geiger-mode-APD-FPAs/10.1117/12.668668.short

[89] A. S. Huntington, M. A. Compton, and G. M. Williams, "Linear-mode single-photon APD detectors," in *Advanced Photon Counting Techniques II*, vol. 6771. International Society for Optics and Photonics, p. 67710Q. [Online]. Available:

https://www.spiedigitallibrary.org/conference-proceedings-of-spie/6771/67710Q/Linear-mode-single-photon-APD-detectors/10.1117/12.751925.short

[90] J. C. Jackson, P. K. Hurley, B. Lane, A. Mathewson, and A. P. Morrison, "Comparing leakage currents and dark count rates in Geiger-mode avalanche photodiodes," vol. 80, no. 22, pp. 4100–4102. [Online]. Available: https://aip.scitation.org/doi/abs/10.1063/1.1483119

[91] M. E. Grein, A. J. Kerman, E. A. Dauler, O. Shatrovoy, R. J. Molnar, D. Rosenberg, J. Yoon, C. E. DeVoe, D. V. Murphy, B. S. Robinson, and D. M. Boroson, "Design of a ground-based optical receiver for the lunar laser communications demonstration," in *2011 International Conference on Space Optical Systems and Applications (ICSOS)*, pp. 78–82.

[92] H. Shibata, T. Honjo, and K. Shimizu, "Quantum key distribution over a 72 dB channel loss using ultralow dark count superconducting single-photon detectors," vol. 39, no. 17, pp. 5078–5081. [Online]. Available: https://www.osapublishing.org/ol/abstract.cfm?uri=ol-39-17-5078

[93] H. Shibata, K. Fukao, N. Kirigane, S. Karimoto, and H. Yamamoto, "SNSPD with Ultimate Low System Dark Count Rate Using Various Cold Filters," vol. PP, pp. 1–1.

[94] S. Chen, L. You, W. Zhang, X. Yang, H. Li, L. Zhang, Z. Wang, and X. Xie, "Dark counts of superconducting nanowire single-photon detector under illumination," vol. 23, no. 8, p. 10786. [Online]. Available: https://www.osapublishing.org/abstract.cfm?URI=oe-23-8-10786

[95] C. Liu, S. Chen, X. Li, and H. Xian, "Performance evaluation of adaptive optics for atmospheric coherent laser communications," vol. 22, no. 13, pp. 15 554–15 563. [Online]. Available: https://www.osapublishing.org/oe/abstract.cfm?uri=oe-22-13-15554

[96] L. C. Roberts, J. E. Roberts, S. F. Fregoso, T. N. Truong, H. Herzog, G. L. Block, J. D. Rodriguez, S. R. Meeker, and J. A. Tesch, "A laser communication adaptive optics system as a testbed for extreme adaptive optics," in *Adaptive Optics Systems VI*, D. Schmidt, L. Schreiber, and L. M. Close, Eds. SPIE, p. 65. [Online]. Available: https://www.spiedigitallibrary.org/conference-proceedings-of-spie/10703/2314304/A-laser-communication-adaptive-optics-system-as-a-testbed-for/10.1117/12.2314304.full

[97] T. C. Farrell, "The effect of atmospheric optical turbulence on laser communications systems: Part 1, theory," in *Sensors and Systems for Space Applications XII*, vol. 11017. International Society for Optics and Photonics, p. 110170B. [Online]. Available: https://www.spiedigitallibrary.org/conference-proceedings-of-spie/11017/110170B/The-effect-of-atmospheric-optical-turbulence-on-laser-communications-systems/10.1117/12.2520055.short

[98] M. W. Wright, J. Kovalik, J. Morris, M. Abrahamson, and A. Biswas, "LEO-to-ground optical communications link using adaptive optics correction on the OPALS downlink," in *Free-Space Laser Communication and Atmospheric Propagation XXVIII*, vol. 9739. International Society for Optics and Photonics, p. 973904. [Online]. Available: https://www.spiedigitallibrary.org/conference-proceedings-of-spie/9739/973904/LEO-to-ground-optical-communications-link-using-adaptive-optics-correction/10.1117/12.2211201.short

[99] L. C. Roberts, R. Burruss, S. Fregoso, H. Herzog, S. Piazzola, J. E. Roberts, G. D. Spiers, and T. N. Truong, "The adaptive optics and transmit system for NASA's Laser Communications Relay Demonstration project," A. M. J. van Eijk, C. C. Davis, and S. M. Hammel, Eds., p. 99790I. [Online]. Available: http://proceedings.spiedigitallibrary.org/proceeding.aspx?doi=10.1117/12.2238589

[100] L. Andrej, F. Perecar, J. Jaros, M. Papes, P. Koudelka, J. Latal, J. Cubik, and V. Vasinek, "Features and range of the FSO by use of the OFDM and QAM modulation in different atmospheric conditions," in *Wireless Sensing, Localization, and Processing IX*, vol. 9103. International Society for Optics and Photonics, p. 91030O. [Online]. Available: https://www.spiedigitallibrary.org/conference-proceedings-of-spie/9103/91030O/Features-and-range-of-the-FSO-by-use-of-the/10.1117/12.2050279.short

[101] M. Stevens, D. Boroson, and D. Caplan, "A novel variable-rate pulse-position modulation system with near quantum limited performance," in *1999 IEEE LEOS Annual Meeting Conference Proceedings. LEOS'99. 12th Annual Meeting. IEEE Lasers and Electro-Optics Society 1999 Annual Meeting (Cat. No.99CH37009)*, vol. 1, pp. 301–302 vol.1.

[102] M. M. Willis, A. J. Kerman, M. E. Grein, J. Kansky, B. R. Romkey, E. A. Dauler, D. Rosenberg, B. S. Robinson, D. V. Murphy, and D. M. Boroson, "Performance of a Multimode Photon-Counting Optical Receiver for the NASA Lunar Laser Communications Demonstration," p. 3.

[103] W. T. Roberts, D. Antsos, A. Croonquist, S. Piazzolla, L. C. R. Jr, V. Garkanian, T. Trinh, M. W. Wright, R. Rogalin, J. Wu, and L. Clare, "Overview of Ground Station 1 of the NASA space communications and navigation program," in *Free-Space Laser Communication and Atmospheric Propagation XXVIII*, vol. 9739. International Society for Optics and Photonics, p. 97390B. [Online]. Available: https://www.spiedigitallibrary.org/conference-proceedings-of-spie/9739/97390B/Overview-of-Ground-Station-1-of-the-NASA-space-communications/10.1117/12.2217465.short

[104] J. M. Kahn, "Modulation and Detection Techniques for Optical Communication Systems," in *Optical Amplifiers and Their Applications/Coherent Optical Technologies and Applications*. OSA, p. CThC1. [Online]. Available: https://www.osapublishing.org/abstract.cfm?URI=COTA-2006-CThC1

[105] *Fiber Optic Measurement Techniques*. Elsevier. [Online]. Available: https://linkinghub.elsevier.com/retrieve/pii/B9780123738653X00018

[106] B. Smutny and R. Lange, "Homodyne BPSK Based Optical Inter-Satellite Communication Links," in *24th AIAA International Communications Satellite Systems Conference*. American Institute of Aeronautics and Astronautics. [Online]. Available: http://arc.aiaa.org/doi/10.2514/6.2006-5460

[107] J. B. Padhy and B. Patnaik, "Optical Wireless Systems with DPSK and Manchester Coding," in *Smart and Innovative Trends in Next Generation Computing Technologies*, ser. Communications in Computer and Information Science, P. Bhattacharyya, H. G. Sastry, V. Marriboyina, and R. Sharma, Eds. Springer, pp. 155–167.